JOC The Journal of Organic Chemistry

Article

pubs.acs.org/joc

Mechanistic Investigation on the Formation of 2-Halo-3-aryl-4(3*H*)-quinazoliniminium Halides from Heteroenyne-allenes: A Computational Study

Pamela S. Filby and Sundeep Rayat*

Department of Chemistry, Ball State University, Cooper Physical Science Building, Muncie, Indiana 47304−0445, United States

Supporting Information

ABSTRACT: Intramolecular cyclization of the heteroenyne-allene, 2-((phenylimino)methyleneamino)-benzonitrile (**1**) in the presence of HCl to produce 2-chloro-3-phenyl-4(3*H*)-quinazoliniminium chloride (**Qz**) involves the formation of two new bonds: a C−Cl bond and a C−N bond. We propose five pathways for this reaction. Four of these pathways involve chloride capture to form the C−Cl bond prior to the intramolecular nucleophilic attack to form the C−N bond, while one pathway involves ring closure to form the C−N bond prior to C−Cl bond formation. All calculations were carried out at B3LYP and MP2 levels of theory and employed the 6-311G* basis set. The solvent effects were considered using a Polarized Continuum Model with dichloromethane as the solvent. The calculations at both levels show that the mechanism involves initial protonation of **1**, preferentially at N_α to give **2** which rapidly captures the chloride ion to form **5**. This intermediate is protonated at the −CN group to form **8ROT**, which then tautomerizes to its more stable isomer **9ROT**. The latter undergoes intramolecular nucleophilic attack from N_β to the protonated −CN group to form the cyclized intermediate **12**, which tautomerizes to its most stable isomer **13**. The coordination of Cl^- ion present in the solution with **13** gives the final product **Qz**.

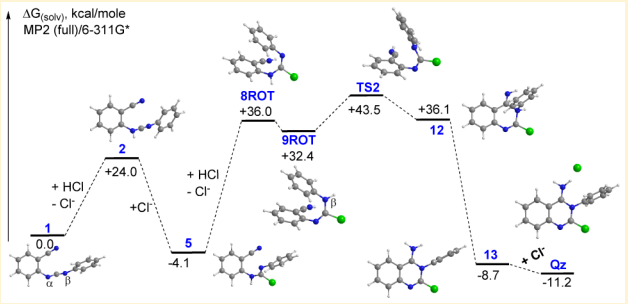

INTRODUCTION

Natural and synthetic compounds containing the 4(3*H*)-quinazolinone ring system exhibit a broad range of applications in medicine as antihypertensive,[1] antimalarial,[2] antimicrobial,[3] anticonvulsive,[4] anti-Alzheimer's,[5] antiarteriosclerotic,[6] anti-cancer,[7] anti-inflammatory,[8] and analgesic[9] agents (Figure 1). 4(3*H*)-Quinazolinones have also found uses in industry as electroluminescent materials and dyes.[10] As a result, there is a continued demand for the search and discovery of new, efficient, and versatile methods to synthesize these molecular frameworks.[11] One way to obtain the 4(3*H*)-quinazolinone scaffold is from 4(3*H*)-quinazolinimine, which is considered to be an important building block of the quinazolinone ring system. Some synthetically produced 4(3*H*)-quinazolinimines have also demonstrated therapeutic potential against Alzheimer's disease and cancer (Figure 1).[12] Therefore, several synthetic methods have been developed for the construction of this latter framework.[13] However, most of these protocols suffer from low product yields,[12c,14] lack of versatility,[15] high temperature requirements,[16] tedious workup conditions,[12b,13a,b,17] and long reactions times.[18]

Our research group has reported a facile synthetic route to obtain the 4(3*H*)-quinazoliniminium scaffold, specifically, the 2-chloro-3-phenyl-4(3*H*)-quinazoliniminium chloride salt (**Qz**) through the intramolecular cyclization of heteroenyne-allene **1** in the presence of chlorotrimethylsilane (TMSCl) and trace water with dichloromethane as solvent at room temperature[19] (Scheme 1). It was believed that the reaction involves the generation of HCl *in situ*, from TMSCl and trace water, which plays an important role toward product formation. To confirm this hypothesis, HCl gas was passed through a solution of **1** dissolved in dichloromethane at room temperature, and this indeed resulted in the formation of **Qz**.[19] The reaction is highly versatile, and several derivatives of **Qz** carrying a variety of electron donating and electron withdrawing groups on the aromatic rings were prepared from the corresponding heteroenyne-allenes by this method in good to excellent yields.[19] No other products were detected in our reaction mixture. The cyclization of **1** to **Qz** involves (a) C−Cl bond formation and (b) an intramolecular C−N bond formation. The sequence in which these two events take place was not known. In this article, we undertook a computational study to gain insights into the mechanism of cyclization of **1** to **Qz** with the goal of identifying critical reactive intermediates involved in the formation of the product, which could subsequently enable us to select, modify, or/and improve experimental conditions to increase the efficiency and scope of this reaction. In addition, the investigation of the mechanism of **Qz** formation may direct efforts toward the exploration of new chemistry emanating from the putative reactive intermediates and thus expand a synthetic chemist's toolbox of useful reactions.

Received: November 21, 2014
Published: April 13, 2015

DOI: 10.1021/jo502664s
J. Org. Chem. 2015, 80, 4299−4305

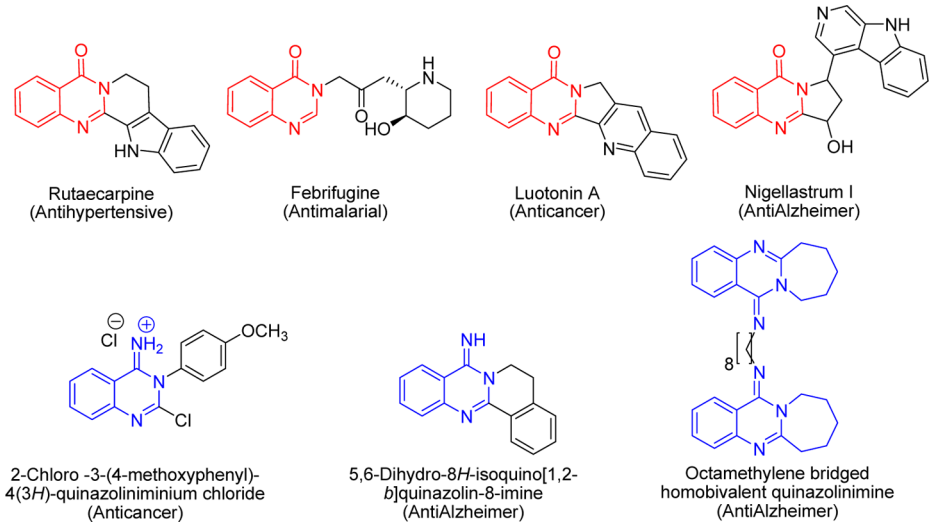

Figure 1. Select examples featuring the 4(3*H*)-quinazolinone (red) and 4(3*H*)-quinazolinimine (blue) cores.

Scheme 1. 2-Chloro-3-phenyl-4(3*H*)-quinazoliniminium Chloride (Qz) from Heteroenyne-allene 1

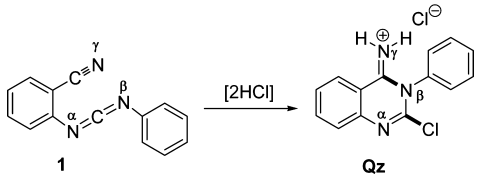

Note that the cyclization under study is in stark contrast to the well-known thermally and photochemically triggered Myers-Saito (C^2-C^7)[20] and Schmittel (C^2-C^6)[21] cyclizations of the related systems, e.g., enyne-allenes and enyne-carbodimides, which involve diradical[22] or carbene intermediates,[23] and lead to the formation of completely different products arising through H atom abstraction from a suitable H-donor,[20a] formal ene reaction,[21a] formal Diels–Alder,[24] or formal [2 + 2] reactions.[25] Similar thermal and photochemical cyclizations of **Qz** have been investigated in our laboratory but were unsuccessful.

Scheme 2. Proposed Mechanistic Pathways for the Addition of HCl to Heteroenyne-allene 1 to form Qz

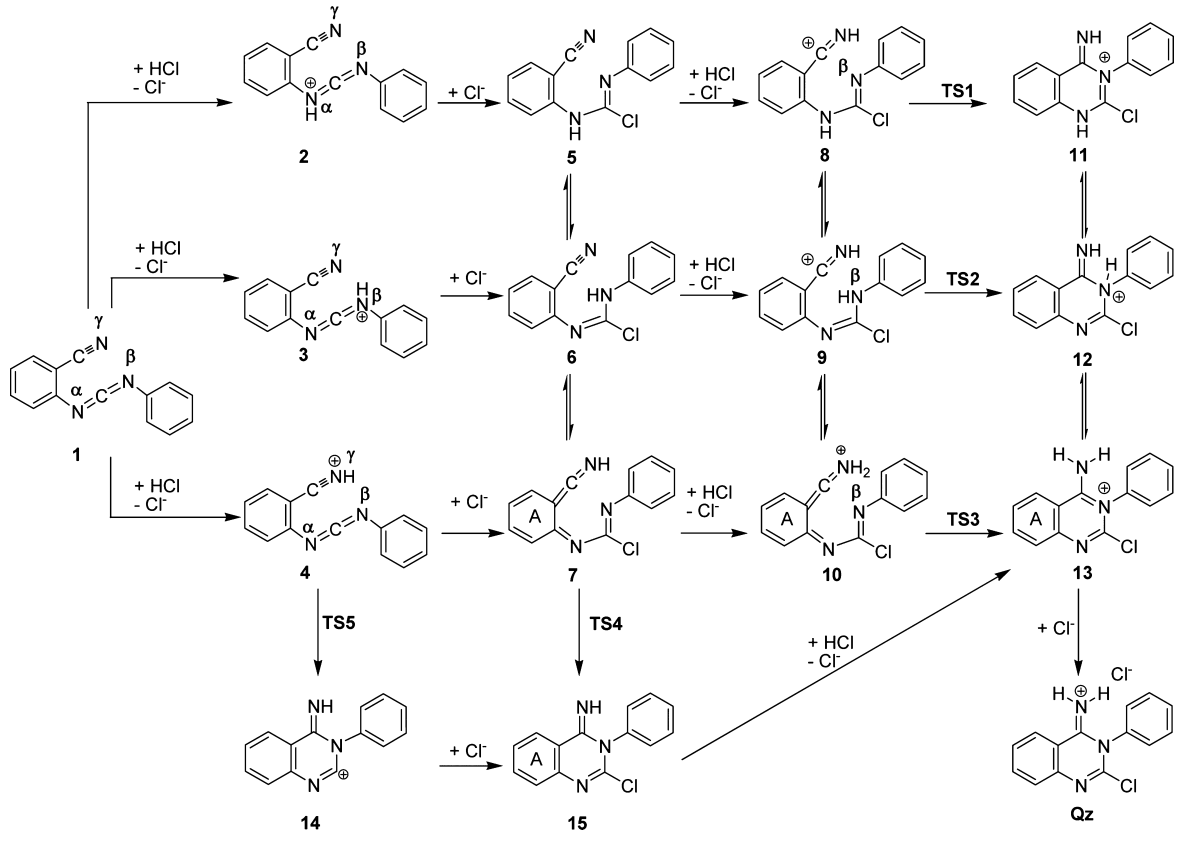

DOI: 10.1021/jo502664s
J. Org. Chem. 2015, 80, 4299–4305

COMPUTATIONAL METHODS

All calculations were performed using the Gaussian 09 package of programs.[26] Optimized geometries of all stationary points on the potential energy surface were first obtained using density functional theory (B3LYP) with the employment of the 6-311G*[27] basis set. Optimizations were followed with vibrational analyses to ensure an imaginary frequency of zero for the ground states and one for the transition states.[28] Solvent effect on the reaction energies and activation barriers was considered by performing single point polarized continuum model (PCM)[29] calculations for dichloromethane (ε = 8.93) on optimized gas phase geometries at B3LYP/6-311G*. Although, DFT is a widely used cost-effective method for routine computations of large molecular systems, it has been shown to be inadequate in describing the conjugated π-bonded systems and their proton affinities.[30] The inaccuracy of the DFT is attributed to the self-interaction error.[31] Therefore, the potential energy surface was also mapped at second order MØller−Plesset perturbation theory (MP2(full))[32] using the 6-311G* basis set. Vibrational data were obtained to characterize the minima (zero imaginary frequency) and transition states (one negative (imaginary) frequency). Solvent effects were considered by performing single point PCM[29] calculations for dichloromethane (ε = 8.93) on optimized gas phase geometries at MP2(full)/6-311G*. **TS3** cannot be located at the MP2 level (vide infra).

Each transition state connecting the corresponding reactant and product was confirmed by following the intrinsic reaction coordinate[33] (IRC) path in both directions. For **TS1**, **TS2**, **TS4**, and **TS5**, the IRC analyses were carried out at MP2, and for **TS3**, this calculation was performed at the B3LYP level of theory. Thermochemical data obtained in gas phase at both levels was used with the corresponding single point solvation energies to calculate Gibbs free energies of solvation. Both B3LYP and MP2 produced identical overall conclusions about the mechanistic pathway. However, the reaction was predicted to be more exothermic at the MP2 level and exhibited slightly lower energetic requirements to form the product as opposed to the B3LYP level (Figures 5S and 6S, Supporting Information). The discussion below is based on $\Delta G_{(solv)}$ at MP2(full)/6-311G*.

RESULTS AND DISCUSSION

The reaction of heteroenyne-allene **1** with HCl to form the 2-chloro-3-phenyl-4(3*H*)-quinazoliniminium chloride salt (**Qz**)

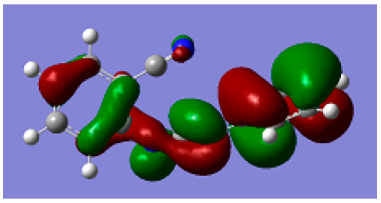

Figure 2. HOMO of heteroenyne-allene 1.

may involve any of the five possible pathways depicted in Scheme 2. After the initial protonation at N_α, N_β, and N_γ to form intermediates **2**, **3**, and **4**, four of the pathways consider Cl^- capture at the carbodiimide carbon (C−Cl bond formation) prior to the nucleophilic attack of N_β on the protonated −CN group (C−N bond formation) involving intermediates **5**, **6**, and **7**, and one considers nucleophilic attack prior to the Cl^- capture via intermediate **14**. These pathways are discussed in the following sections.

Protonation of Heteroenyne-allene 1. In the presence of a Bronsted acid (HCl), there are three possible sites for the protonation of **1**, i.e., at N_α, N_β, and N_γ. The highest occupied molecular orbital (HOMO) of heteroenyne-allene **1** was analyzed to determine the preferred sites of protonation

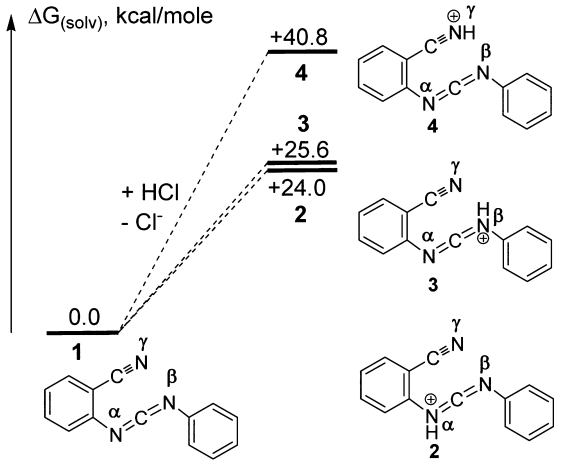

Figure 3. Protonation of heteroenyne-allene.

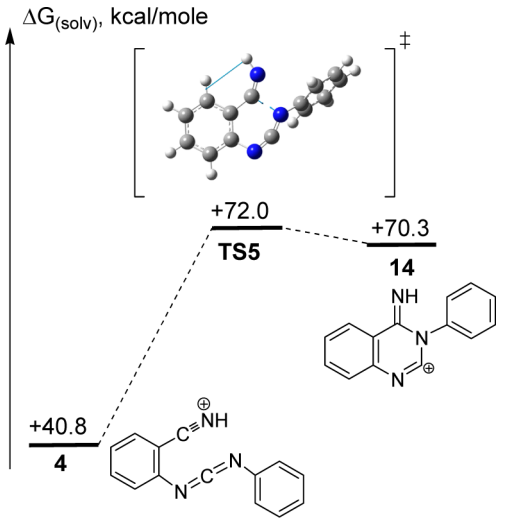

Figure 4. Intramolecular cyclization of **4** (energies are relative to **1**). Displacement vectors for **TS5** are also shown.

(Figure 2). Note that the molecular orbital component is mostly localized on the carbodiimide moiety (-N=C=N-) and on the phenyl ring attached to the N_β. There is no contribution of the molecular orbital on the −CN group. This implies that N_α and N_β of **1** are more basic than N_γ and are therefore expected to undergo faster protonation. This hypothesis is also supported by literature precedence that reports carbodiimides to exhibit higher proton affinities than nitriles.[34]

Indeed, our data indicate that protonation of **1** at N_α to form **2** (24.0 kcal/mol) and at N_β to form **3** (25.6 kcal/mol) is more favorable than protonation at N_γ to give **4** (40.8 kcal/mol) as shown in Figure 3. There is also not a significant difference in the $\Delta G_{(solv)}$ values for the protonation of N_α and N_β, even though the frontier molecular orbital theory suggests N_β to be more basic than N_α and hence more likely to get protonated (Figure 2).

Intramolecular Nucleophilic Attack Prior to Chloride Capture. The above result implies that **4** is a high energy intermediate and that any further chemistry emanating from this species is expected to have a minor contribution. In fact, the pathway that considers intramolecular nucleophilic attack (C−N bond formation) in **4** to form **14** via **TS5** prior to chloride capture (C−Cl bond formation) is extremely ender-

DOI: 10.1021/jo502664s
J. Org. Chem. 2015, 80, 4299−4305

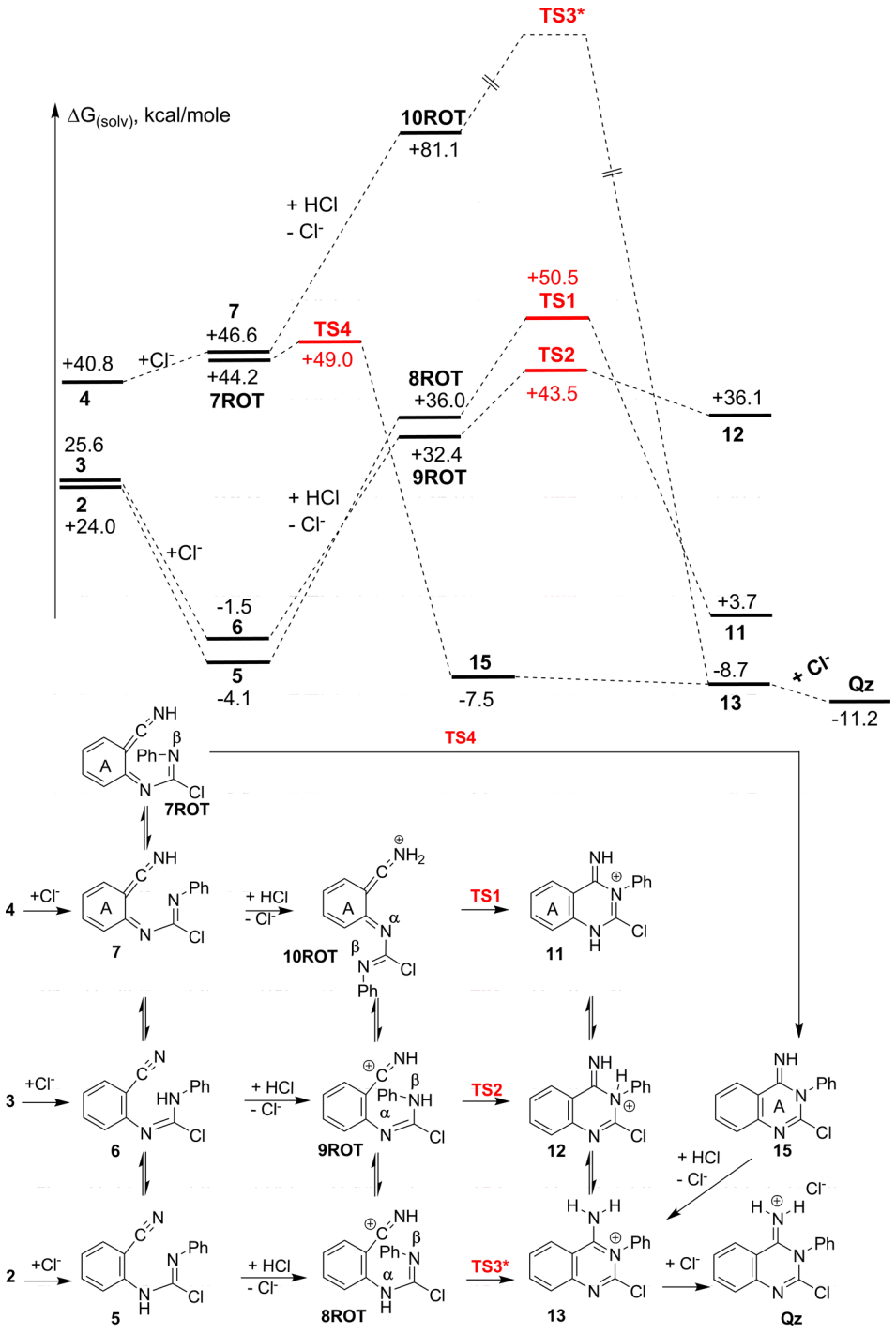

Figure 5. Cl^- capture by **2**–**4** followed by protonation and cyclization to product formation. Energies are relative to heteroenyne-allene **1**.

gonic (29.5 kcal/mol) and is associated with a large activation barrier of 31.2 kcal/mol (72.0 kcal/mol from **1**). Thus, this pathway is not expected to play any significant role in the mechanism (Figure 4).

Chloride Capture Prior to Intramolecular Nucleophilic Attack. The capture of Cl^- at the carbodiimide carbon to form **5**, **6**, and **7**, is a highly exergonic process for **2** and **3** ($\Delta G_{(solv)}$ values of −28.1 and −27.1 kcal/mol, respectively); however, it is slightly endergonic for **4** (5.8 kcal/mol) owing to the loss of aromaticity in ring A of **7** (Figure 5). Next, as outlined in Scheme 2, the protonation of **5**–**7** is expected to form cations **8**–**10**. However, the attempted optimization of intermediates **8**–**10** with the phenyl ring attached to N_β, syn to the C–Cl bond, resulted in cyclization to the corresponding cations **11**–**13**. This is attributed to the presence of a protonated nitrile group in close proximity to the nucleophilic nitrogen atom (N_β). Instead, we were able to obtain the rotamers **8ROT** and **9ROT** in which the phenyl ring attached to N_β is anti to the C–Cl bond and **10ROT** with an "*E*" configuration about the C=N_α bond (Figure 6). The protonation of **5**–**7** at the nitrile group to form intermediates **8ROT**–**10ROT** occurs with a free energy increase of 40.1, 33.9, and 34.5 kca1/mol, respectively.

The protonation of the −CN group activates **8ROT**, **9ROT**, and **10ROT** toward nucleophilic attack[35] from N_β of the

DOI: 10.1021/jo502664s
J. Org. Chem. 2015, 80, 4299–4305

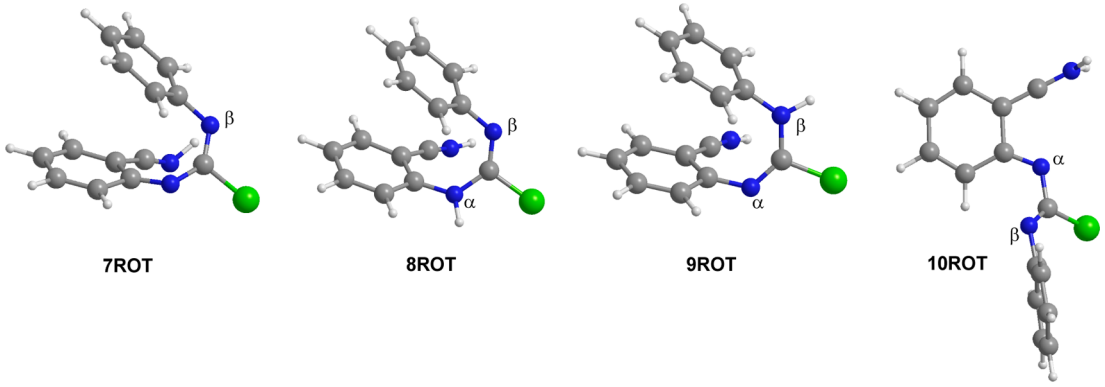

Figure 6. Optimized structures of **7ROT**−**10ROT** at MP2(full)/6-311G*.

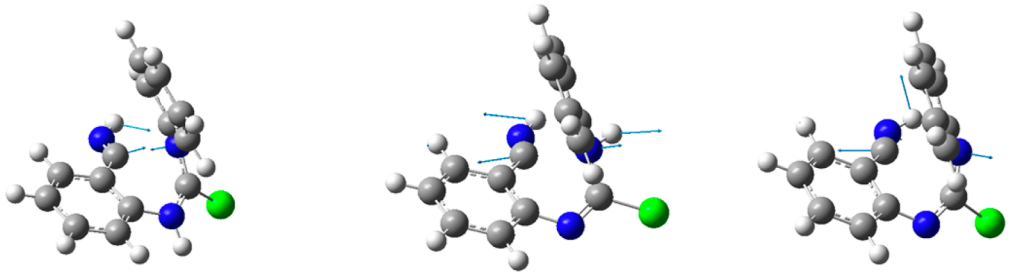

Figure 7. Optimized structures of **TS1** (left), **TS2** (center), and **TS4** (right) at MP2(full)/6-311G* (displacement vectors are also shown).

carbodiimide moiety. This nucleophilic attack in the case of **8ROT** and **9ROT** leads to the formation of the ring cyclized cations **11** and **12** via **TS1** and **TS2**, respectively (Figure 7). The conversion of **8ROT** to **11** is highly exergonic (−32.3 kcal/mol) and occurs with an activation barrier of 14.5 kcal/mol. However, the conversion of **9ROT** to **12** is endergonic (3.7 kcal/mol) and occurs with a slightly lower activation barrier of 11.1 kcal/mol (Figure 5). The cyclization of **10ROT** to **13** occurs with an 89.8 kcal/mol free energy decrease. We were unable to obtain the transition state **TS3** at the MP2 level. At B3LYP, **TS3** was found to have a high activation barrier of 31.7 kcal/mol (+103.8 kcal/mol from **1**) from the corresponding B3LYP/6-311G* optimized **10ROT** in dichloromethane as solvent using the PCM model (Figure 6S, Supporting Information). IRC analysis revealed that as **10ROT** undergoes rotational isomerism to **10** at room temperature, it undergoes ring closure to form **13** via **TS3** (Figures 3S, 5S, and 6S, Supporting Information).

One other pathway for C−N bond formation involves electrocyclization of **7** to **15**. We were able to locate the transition state structure **TS4** connecting the rotamer **7ROT** to **15** (Figure 7). **7ROT**, which has a phenyl ring at N_{β}, anti to the C−Cl bond similar to **8ROT**−**10ROT**, is 2.4 kcal/mol more stable than **7**. This path is strongly exergonic (−51.7 kcal/mol) due to the regaining of aromaticity in ring A of product **15** and is calculated to proceed with a small activation barrier of 4.8 kcal/mol (Figure 5).

Tautomerization between the Pathways. Because of the significantly high activation barrier associated with pathway **1** → **4** → **7**(**7ROT**) → **10ROT** → **TS3** → **13**, it is not expected to contribute toward the formation of the final product **Qz**. However, the pathways **1** → **2** → **5** → **8ROT** → **TS1** → **11** → **Qz**, **1** → **3** → **6** → **9ROT** → **TS2** → **12** → **Qz**, and **1** → **4** → **7ROT** → **TS4** → **15** → **13** → **Qz** have essentially identical energy requirements with the highest energy point on these at +50.5 (**TS1**), +43.5 (**TS2**), and +49.0 (**TS4**) kcal/mol, respectively (Figure 5). Therefore, it is not possible to favor one of these pathways over the others based on energetics. However, one important aspect of this cyclization reaction is that the various pathways are interconnected via tautomerization (Scheme 2 and Figure 5, bottom). For instance, **5**−**7**(**7ROT**) are interconverting tautomers with **5** being most stable and **6** only 2.6 kcal/mol higher in energy. However, **7** and its rotamer **7ROT** are 50.7 and 48.3 kcal/mol more unstable than **5**. Similarly, among **8ROT**−**10ROT**, **9ROT** is the most stable tautomer, with **8ROT** and **10ROT** about 3.6 and 48.7 kcal/mol higher in energy, respectively. The high energy associated with **7**, **7ROT**, and **10ROT** is attributed to the lack of aromatic character in ring A. In addition, **11**, **12**, and **13** are also tautomers, with **13** being most stable. Compounds **11** and **12** are 12.4 and 44.8 kcal/mol higher in energy than **13**.

Because of the occurrence of this tautomerization between the intermediates, the final mechanistic pathway is predicted to involve the initial protonation of **1**, preferentially at N_{α}, to give **2** that is expected to rapidly capture the chloride ion to form **5**. This intermediate is protonated at the −CN group to form **8ROT**, which then tautomerizes to its more stable isomer **9ROT**. The latter undergoes intramolecular nucleophilic attack from N_{β} to the protonated −CN group to form the cyclized intermediate **12** that tautomerizes to the most stable isomer **13**. The coordination of Cl^- ion present in the solution with **13** gives the final product **Qz** (−2.5 kcal/mol).

■ CONCLUSIONS

We have employed computational methods to investigate the mechanism of formation of 2-chloro-3-phenyl-4(3*H*)-quinazoliniminium chloride salt (**Qz**) from the heteroenyne-allene **1** in the presence of dichloromethane. Our results indicate that the addition of Cl^- to the carbodiimide moiety to form the C−Cl

DOI: 10.1021/jo502664s
J. Org. Chem. 2015, 80, 4299−4305

bond precedes the nucleophilic attack from N_β on the protonated −CN group to form the C−N bond. Furthermore, our calculations suggest that the reaction mechanism follows the pathway **1** → **2** → **5** → **8ROT** → **9ROT** (via tautomerism) → **TS2** → **12** → **13** (via tautomerism) → **Qz**. Overall, the formation of product **Qz** is predicted to occur with 11.2 kcal/mol free energy decrease from the heteroenyne-allene **1** at MP2/6-311G*.

Our mechanistic study further reveals that the protonation of N_α and N_β of **1** occurs in preference to N_γ, which offers the opportunity to explore new chemistry by trapping the intermediates **2** and **3** with an appropriately placed internal nucleophile. As a result, we synthesized heteroenyne-allenes (analogous to **1**) substituted with a biphenyl ring at N_β and successfully cyclized these compounds to phenanthridine fused quinazoliniminiums in the presence of hydrogen halide.[36] The preliminary investigations suggest that the reaction proceeds via the initial protonation of carbodiimide nitrogens to form intermediates similar to **2** and **3**, which are then trapped by a nucleophilic attack from the neighboring biphenyl ring to form the phenanthridinylium cation, which eventually forms the fused heterocycle via a nucleophilic attack on the −CN group. This work will be reported in due course.

■ ASSOCIATED CONTENT

Supporting Information

Optimized structures of the reactants, intermediates, transition states, and products at the B3LYP level, and of minima at the MP2 level; gas phase free energy diagram at both levels and free energy diagram in dichloromethane at B3LYP/6-311G*; total energies and vibrational data of all optimized structures, and single point PCM energies at both levels; optimized Cartesian coordinates of relevant structures at MP2 and at B3LYP. This material is available free of charge via the Internet at http://pubs.acs.org.

■ AUTHOR INFORMATION

Corresponding Author

*E-mail: srayat@bsu.edu.

Notes

The authors declare no competing financial interest.

■ ACKNOWLEDGMENTS

We acknowledge the College of Sciences and Humanities Beowulf Cluster at Ball State University funded by the Office of Sponsored Program for computational time and support.

■ REFERENCES

(1) Chen, Z.; Hu, G.; Li, D.; Chen, J.; Li, Y.; Zhou, H.; Xie, Y. *Bioorg. Med. Chem.* **2009**, *17*, 2351.

(2) (a) Hirai, S.; Kikuchi, H.; Kim, H.-S.; Begum, K.; Wataya, Y.; Tasaka, H.; Miyazawa, Y.; Yamamoto, K.; Oshima, Y. *J. Med. Chem.* **2003**, *46*, 4351. (b) Zhu, S.; Wang, J.; Chandrashekar, G.; Smith, E.; Liu, X.; Zhang, Y. *Eur. J. Med. Chem.* **2010**, *45*, 3864.

(3) Gudasi, K. B.; Shenoy, R. V.; Vadavi, R. S.; Patil, M. S.; Patil, S. A. *Indian J. Chem., Sect. A: Inorg., Bio-inorg., Phys., Theor. Anal. Chem.* **2005**, *44A*, 2247.

(4) Bhandari, S. V.; Deshmane, B. J.; Dangare, S. C.; Gore, S. T.; Raparti, V. T.; Khachane, C. V.; Sarkate, A. P. *Pharmacologyonline* **2008**, 604.

(5) Zheng, X.-y.; Zhang, Z.-j.; Chou, G.-x.; Wu, T.; Cheng, X.-m.; Wang, C.-h.; Wang, Z.-t. *Arch. Pharm. Res.* **2009**, *32*, 1245.

(6) Koyama, N.; Inoue, Y.; Sekine, M.; Hayakawa, Y.; Homma, H.; Oinmura, S.; Tomoda, H. *Org. Lett.* **2008**, *10*, 5273.

(7) (a) Al-Obaid, A. M.; Abdel-Hamide, S. G.; El-Kashef, H. A.; Abdel-Aziz, A. A. M.; El-Azab, A. S.; Al-Khamees, H. A.; El-Subbagh, H. I. *Eur. J. Med. Chem.* **2009**, *44*, 2379. (b) Cinelli, M. A.; Morrell, A.; Dexheimer, T. S.; Scher, E. S.; Pommier, Y.; Cushman, M. *J. Med. Chem.* **2008**, *51*, 4609.

(8) Giri, R. S.; Thaker, H. M.; Giordano, T.; Williams, J.; Rogers, D.; Sudersanam, V.; Vasu, K. K. *Eur. J. Med. Chem.* **2009**, *44*, 4783.

(9) Sindrup, S. H.; Graf, A.; Sfikas, N. *Eur. J. Pain* **2006**, *10*, 567.

(10) (a) Nakatsuka, M.; Ishida, T.; Shimamura, T. JP 2000-209223 2002025775, 2002. (b) Nakatsuka, M.; Kitahon, N. JP 1997-100210 10294178, 1998. (c) Stoessel, P.; Breuning, E.; Joosten, D. WO 2010-EP5857 2011044988, 2011. (d) Patel, D. R.; Patel, K. C. *Fibers Polym.* **2010**, *11*, 537. (e) Patel, D. R.; Patel, K. C. *Fibers Polym.* **2011**, *12*, 741.

(11) Connolly, D. J.; Cusack, D.; O'Sullivan, T. P.; Guiry, P. J. *Tetrahedron* **2005**, *61*, 10153.

(12) (a) Perchellet, J.-P. H.; Waters, A. M.; Perchellet, E. M.; Naganaboina, V. K.; Chandra, K. L.; Desper, J.; Rayat, S. *Anticancer Res.* **2011**, *31*, 2083. (b) Decker, M.; Krauth, F.; Lehmann, J. *Bioorg. Med. Chem.* **2006**, *14*, 1966. (c) Decker, M. *J. Med. Chem.* **2006**, *49*, 5411.

(13) (a) Chen, X.; Tikhonova, I. G.; Decker, M. *Bioorg. Med. Chem.* **2011**, *19*, 1222. (b) Darras, F. H.; Kling, B.; Heilmann, J.; Decker, M. *ACS Med. Chem. Lett.* **2012**, *3*, 914. (c) Qiu, G.; Liu, G.; Pu, S.; Wu, J. *Chem. Commun.* **2012**, *48*, 2903.

(14) Lettau, H.; Buege, A.; Harenberg, P.; Haertel, S.; Jarmer, K.; Kock, K.; Poeppel, W.; Schikora, A.; Schneider, R.; et al. *Pharmazie* **1993**, *48*, 410.

(15) Szczepankiewicz, W.; Suwinski, J.; Bujok, R. *Tetrahedron* **2000**, *56*, 9343.

(16) Jaen, J. C.; Gregor, V. E.; Lee, C.; Davis, R.; Emmerling, M. *Bioorg. Med. Chem. Lett.* **1996**, *6*, 737.

(17) Decker, M. *Eur. J. Med. Chem.* **2005**, *40*, 305.

(18) Szczepankiewicz, W.; Suwinski, J. *Chem. Heterocycl. Compd.* **2001**, *36*, 809.

(19) Naganaboina, V. K.; Chandra, K. L.; Desper, J.; Rayat, S. *Org. Lett.* **2011**, *13*, 3718.

(20) (a) Myers, A. G.; Kuo, E. Y.; Finney, N. S. *J. Am. Chem. Soc.* **1989**, *111*, 8057. (b) Nagata, R.; Yamanaka, H.; Okazaki, E.; Saito, I. *Tetrahedron Lett.* **1989**, *30*, 4995.

(21) (a) Schmittel, M.; Strittmatter, M.; Kiau, S. *Tetrahedron Lett.* **1995**, *36*, 4975. (b) Schmittel, M.; Keller, M.; Kiau, S.; Strittmatter, M. *Chem.—Eur. J.* **1997**, *3*, 807.

(22) (a) Bucher, G.; Mahajan, A. A.; Schmittel, M. *J. Org. Chem.* **2008**, *73*, 8815. (b) Bucher, G.; Mahajan, A. A.; Schmittel, M. *J. Org. Chem.* **2009**, *74*, 5850.

(23) Schmittel, M.; Steffen, J.-P.; Rodriguez, D.; Engelen, B.; Neumann, E.; Cinar, M. E. *J. Org. Chem.* **2008**, *73*, 3005.

(24) (a) Schmittel, M.; Strittmatter, M.; Vollmann, K.; Kiau, S. *Tetrahedron Lett.* **1996**, *37*, 999. (b) Schmittel, M.; Kiau, S.; Siebert, T.; Strittmatter, M. *Tetrahedron Lett.* **1996**, *37*, 7691.

(25) Cinar Mehmet, E.; Vavilala, C.; Fan, J.; Schmittel, M. *Org. Biomol. Chem.* **2011**, *9*, 3776.

(26) Frisch, M. J.; Trucks, G. W.; Schlegel, H. B.; Scuseria, G. E.; Robb, M. A.; Cheeseman, J. R.; Scalmani, G.; Barone, V.; Mennucci, B.; Petersson, G. A.; Nakatsuji, H.; Caricato, M.; Li, X.; Hratchian, H. P.; Izmaylov, A. F.; Bloino, J.; Zheng, G.; Sonnenberg, J. L.; Hada, M.; Ehara, M.; Toyota, K.; Fukuda, R.; Hasegawa, J.; Ishida, M.; Nakajima, T.; Honda, Y.; Kitao, O.; Nakai, H.; Vreven, T.; Montgomery, J. A., Jr.; Peralta, J. E.; Ogliaro, F.; Bearpark, M.; Heyd, J. J.; Brothers, E.; Kudin, K. N.; Staroverov, V. N.; Kobayashi, R.; Normand, J.; Raghavachari, K.; Rendell, A.; Burant, J. C.; Iyengar, S. S.; Tomasi, J.; Cossi, M.; Rega, N.; Millam, M. J.; Klene, M.; Knox, J. E.; Cross, J. B.; Bakken, V.; Adamo, C.; Jaramillo, J.; Gomperts, R.; Stratmann, R. E.; Yazyev, O.; Austin, A. J.; Cammi, R.; Pomelli, C.; Ochterski, J. W.; Martin, R. L.; Morokuma, K.; Zakrzewski, V. G.; Voth, G. A.; Salvador, P.; Dannenberg, J. J.; Dapprich, S.; Daniels, A. D.; Farkas, Ö.; Foresman, J. B.; Ortiz, J. V.; Cioslowski, J.; Fox, D. J. *Gaussian*; Gaussian Inc.: Wallingford, CT, 2009.

DOI: 10.1021/jo502664s
J. Org. Chem. 2015, 80, 4299−4305

(27) (a) Frisch, M. J.; Pople, J. A.; Binkley, J. S. *J. Chem. Phys.* **1984**, *80*, 3265. (b) Krishnan, R.; Binkley, J. S.; Seeger, R.; Pople, J. A. *J. Chem. Phys.* **1980**, *72*, 650.
(28) All transition states were found to be stable with respect to a restricted→unrestricted perturbation except for transition state **TS3**. A broken symmetry calculation lowered the energy by 11.5 kcal/mol for **TS3**, but since this transition state does not appear to be an energetically relevant pathway, additional calculations were not pursued.
(29) Miertus, S.; Scrocco, E.; Tomasi, J. *Chem. Phys.* **1981**, *55*, 117.
(30) Zhao, Y.; Truhlar, D. G. *J. Phys. Chem. A* **2006**, *110*, 10478.
(31) (a) Cohen, A. J.; Mori-Sanchez, P.; Yang, W. *Chem. Rev.* **2012**, *112*, 289. (b) Perdew, J. P.; Zunger, A. *Phys. Rev. B* **1981**, *23*, 5048.
(32) (a) M?ller, C.; Plesset, M. S. *Phys. Rev.* **1934**, *46*, 618. (b) Head-Gordon, M.; Pople, J. A.; Frisch, M. J. *Chem. Phys. Lett.* **1988**, *153*, 503.
(33) (a) Fukui, K. *Acc. Chem. Res.* **1981**, *14*, 363. (b) Hratchian H. P.; Schlegel, H. B. *Theory and Applications of Computational Chemistry: The First Forty Years*; Elsevier: New York, 2005; p 195 (c) Hratchian, H. P.; Schlegel, H. B. *J. Chem. Theory Comp.* **2005**, *1*, 61. (d) Gonzalez, C.; Schlegel, H. B. *J. Chem. Phys.* **1989**, *90*, 2154.
(34) Elrod, M. J. *Int. J. Mass Spec.* **2003**, *228*, 91.
(35) Cantillo, D.; Gutmann, B.; Kappe, C. O. *J. Org. Chem.* **2012**, *77*, 10882.
(36) Alawode, O. E.; Naganaboina, V. K.; Liyanage, T.; Desper, J.; Rayat, S. *Org. Lett.* **2014**, *16*, 1494.

DOI: 10.1021/jo502664s
J. Org. Chem. 2015, 80, 4299−4305